International Journal of Science and Research (IJSR)
ISSN: 2319-7064
Impact Factor 2025: 7.089

Neutrino Oscillations and the Mass Hierarchy Problem

Prakash Bhushan Kumar[1], Dharmanath Goit[2]

[1]Research Scholar, Dept. of Physics, B.S. College, Danapur, Patna 800012, India
Email: *prakashbhushan1990[at]gmail.com*

Associate Professor of physics, B.S. College, Danapur, Patna 800012, India
Email: *goitdn[at]gmail.com*

Abstract: ***Over the past two decades, one of the most significant breakthroughs in elementary particle physics has been the discovery of neutrino oscillations, a phenomenon that reveals properties of neutrinos extending beyond the Standard Model. Despite this progress, a complete understanding of neutrino oscillations and their implications remains an open challenge. This paper presents the theoretical foundations of neutrino oscillation phenomena and examines the experimental techniques and detectors that have investigated neutrinos originating from diverse sources.***

Keywords: Neutrino oscillation, CP symmetry, Normal Ordering, Inverted Ordering, Mixing angles

1. Introduction

Neutrino studies have led to some of the most significant breakthroughs in particle physics over the past decades. Nevertheless, the properties of neutrinos remain far from fully understood. The discovery of the oscillation phenomenon marked a profound revolution in the Standard Model of elementary particles, providing direct evidence for a nonzero neutrino mass. The concept of neutrino oscillations was first proposed by Pontecorvo in 1957 [1–3], long before any experimental indication of this phenomenon. Following several decades of extensive experimental and theoretical research, many fundamental questions remain unresolved regarding the interpretation of oscillations, the determination of oscillation parameters, the absolute neutrino masses, the mass hierarchy, CP violation in the leptonic sector, and the possible existence of a fourth, sterile neutrino.

The widely accepted Mikheyev–Smirnov–Wolfenstein (MSW) model [4–6] provides a framework for interpreting solar neutrino oscillations. While it has been validated for oscillations in both vacuum and matter, its applicability in the vacuum–matter transition region is not yet fully established. The shape of this transition may be significantly influenced by physics beyond the Standard Model, such as non-standard neutrino interactions or the existence of a very light sterile neutrino. Consequently, the transition region requires further and more refined experimental investigation.

Ongoing and planned experiments are actively probing neutrino oscillations using diverse approaches, including neutrino-flavour disappearance and appearance channels, short- and long-baseline source-to-detector configurations, and measurements of neutrinos and antineutrinos originating from solar, atmospheric, accelerator, geophysical, and reactor sources.

Because neutrinos interact with matter exclusively through the weak interaction, they provide nearly undistorted information about their sources. For instance, the study of solar neutrinos and geoneutrinos yields insights not only into the intrinsic properties of neutrinos but also into the internal structure of the Sun and the Earth.

This paper is organized into five sections. Section 2 reviews the theoretical aspects of neutrino oscillations [7–9]. Section 3 describes analysis of the recent experimental status of neutrino oscillations from the T2K and NOvA experiments. Section 4 summarizes the most important milestones and results achieved in neutrino physics. Finally, we discuss the open problems in the field and outlines expectations for the near future of this exciting area of research.

2. Neutrino Oscillations

In the Standard Model (SM) neutrinos are neutral, massless fermions. They only interact with other particles via weak interactions, which are described by the charged-current (CC) and neutral current (NC) interaction Lagrangians:

$$\mathcal{L}_{CC} = -\frac{g}{2\sqrt{2}} j_\rho^{CC} W^\rho + h.c., \quad \text{-----(1)}$$

$$\mathcal{L}_{NC} = -\frac{g}{2cos\theta_W} j_\rho^{NC} Z^\rho \;, \quad \text{-----(2)}$$

In the above relation, g is the $SU(2)_L$ gauge coupling constant, θ_W is the weak angle, and the charged and neutral currents j_ρ^{CC} and j_ρ^{NC} are given by

$$j_\rho^{cc} = 2\sum_{l=e,\mu,\tau} \bar{\nu}_{lL}\,\gamma_\rho l_L + \cdots, \quad \text{----- (3)}$$

$$j_\rho^{NC} = \sum_{l=e,\mu,\tau} \bar{\nu}_{lL}\,\gamma_\rho \nu_{lL} + \cdots, \quad \text{-----(4)}$$

Where l are the charged lepton fields and we have written only the terms containing the neutrino fields ν_l.

If neutrinos have non-zero masses, the left-handed components $\nu_{\alpha L}$ of the neutrino fields with definite flavour α can be a superposition of the left-handed components ν_{iL} of the neutrino fields with definite masses m_i (in this section we use Greek letters α and β to neutrino flavors and Latin letters i and j to refer to neutrino masses). Assuming that neutrinos are ultra relativistic, we have

$$\nu_{\alpha L} = \sum_{i=1}^{N} U_{\alpha i}\,\nu_{iL} \quad \text{----- (5)}$$

Where U is a unitary matrix. By considering that a field operator creates antiparticles, this implies that a *flavour eigen* *state* $|\nu_\alpha\rangle$ is a superposition of different *mass eigenstates* $|\nu_i\rangle$, according to

$$|\nu_\alpha\rangle = \sum_{i=1}^{N} U_{\alpha i}^{*}\,|\nu_i\rangle\ . \text{ ---------------------------(6)}$$

For antineutrinos, we get

$$|\bar{\nu}_\alpha\rangle = \sum_{i=1}^{N} U_{\alpha i}\,|\bar{\nu}_i\rangle\ . \text{ --------------------------(7)}$$

Theoretically, N, the number of massive neutrinos may be larger than three. In this case, however, we must assume that there are *sterile* neutrinos, that is, light fermions that do not take part in standard weak interactions (1) and (2) and thus are not excluded by LEP results according to which the number of active neutrinos coupled with the $W^{\pm}$ and Z boson is $N_\nu = 2.984 \pm 0.008$ [10].

In the assumption of three massive neutrinos, *the neutrino mixing matrix* U can be expressed in terms of three mixing angles θ_{12}, θ_{23}, and θ_{13}; and one Dirac-type CP phase δ

According to

$$U = R_{23}(\theta_{23})\Gamma(\delta)R_{13}(\theta_{13})\Gamma^{\dagger}(\delta)R_{12}(\theta_{12})\ , \text{ --------(8)}$$

Where $R_{ij}(\theta_{ij})$ represents a Euler rotation by θ_{ij} in the $i\ j$ plane and

$$\Gamma(\delta) = \mathrm{diag}(1,1,e^{i\delta}). \text{ \_\_\_\_\_\_\_\_\_\_\_\_ (9)}$$

We are considering here the assumption that neutrinos are Dirac particles. In the case of Majorana mass terms, the most general form of the mixing matrix contains two additional phases and it is obtained by $U \to U.U_M$, where $U_M = \mathrm{diag}(1, e^{i\phi_1}, e^{i\phi_2})$. [7,8] The Majorana phases ϕ_1 and ϕ_2, however have no observable effects on neutrino oscillations [11]. The mixing matrix U is expressed as

$$U = \begin{pmatrix} c_{12}c_{13} & s_{12}c_{13} & s_{13}e^{-i\delta} \\ -s_{12}c_{23} - c_{12}s_{23}s_{31}e^{i\delta} & c_{12}c_{23} - s_{12}s_{23}s_{31}e^{i\delta} & s_{12}c_{13} \\ s_{12}s_{23} - c_{12}c_{23}s_{31}e^{i\delta} & -c_{12}s_{23} - s_{12}c_{23}s_{31}e^{i\delta} & c_{23}c_{31} \end{pmatrix}, \text{ -------- (10)}$$

Where $c_{ij} = cos\theta_{ij}$ and $s_{ij} = sin\theta_{ij}$. We indicate with $\Delta m_{ij}^2 \equiv m_i^2 - m_j^2$. As it is usually done, we order the neutrino masses such that $\Delta m_{21}^2 > 0$ and $\Delta m_{21}^2 \ll |\Delta m_{31}^2|$. With this choice, the ranges of mixing parameters are determined by

$$0 \le \theta_{12}, \theta_{23}, \theta_{31} \le \frac{\pi}{2}, \quad 0 \le \delta \le 2\pi. \text{ --------- (11)}$$

The sign of Δm_{31}^2 determines the neutrino mass hierarchy, being $\Delta m_{31}^2 > 0$ for normal hierarchy (NH) and $\Delta m_{31}^2 < 0$ for inverted hierarchy (IH).

2.1 Neutrino Evolution Equation

The evolution of a generic neutrino state $|\nu(t)\rangle$ is described by a Schrödinger-like equation

$$i\frac{d|\nu(t)\rangle}{dt} = H|\nu(t)\rangle\ , \text{ -------------------------------- (12)}$$

Where H represents the Hamiltonian operator. The above equation can be expressed in the flavor eigen basis $\{|\nu(t)\rangle\}$. We get

$$i\frac{d\nu^{(f)}(t)}{dt} = H^{(f)}\nu^{(f)}(t), \text{ --------------------------- (13)}$$

Where $\nu^{(f)}(t)$ is the vector describing the flavour content of the neutrino state $|\nu(t)\rangle$ given by

$$\nu^{(f)}(t) = (a_e(t), a_\mu(t), a_\tau(t), \ldots)^T, \text{ ------------ (14)}$$

With $a_\alpha(t) = \langle \nu_\alpha|\nu(t)\rangle$, and the matrix H_f is given by

$$H_{\alpha\beta}^{(f)} = \langle \nu_\alpha|H|\nu_\beta\rangle. \text{ ------------------------------- (15)}$$

In vacuum, the neutrino Hamiltonian H_{vac} is determined in terms of neutrino masses and mixing parameters. We have

$$H_{vac}^{(f)} = UH_{vac}^{(m)}U^{\dagger}, \text{ --------------------------------- (16)}$$

where $H_{vac}^{(m)}$ is the representation for vacuum Hamiltonian in mass eigen basis, given by

$$H_{vac}^{(m)} = \mathrm{diag}\left(\sqrt{\vec{p}^2 + m_1^2}, \ldots \sqrt{\vec{p}^2 + m_N^2}\right)$$

$$\approx |\vec{p}| + \frac{1}{2|\vec{p}|}\mathrm{diag}(m_1^2, \ldots, m_N^2). \text{ ------------------- (17)}$$

In the last equality, we adopted the ultra-relativistic approximation $E \approx |\vec{p}| + \frac{m^2}{2|\vec{p}|}$ and we implicitly assumed that the neutrino state $|\nu(t)\rangle$ can be described as a superposition of states with fixed momentum $\vec{p}$. This corresponds to the so-called *plane wave approximation* which is adequate to describe neutrino evolution when coherence of the different components of the neutrino wave packet is not lost in the detection and propagation processes.[7]

The presence of a matter can affect neutrino propagation in a nontrivial way. In fact, as it was realized by [4], when a neutrino propagates through a medium, its dispersion relation (i.e. energy-momentum relation) is modified by coherent interactions with background particles. This phenomenon, which in optics is accounted for by introducing a refractive index, can be described by adding an effective potential V in the evolution equation, so that

$$i\frac{d|\nu(t)\rangle}{dt} = (H_{vac} + V)|\nu(t)\rangle. \text{ ---------------------------- (18)}$$

In the Standard Model, the effective potential is diagonal in the flavour basis. Thus, we have

$$V^{(f)} = \mathrm{diag}(V_e, V_\mu, V_\tau, 0, \ldots) \text{ ----------------------------- (19)}$$

where we have taken into account that sterile states do not interact with the medium. At low energies, the potentials can be evaluated by taking the average $\langle \mathcal{H}_{eff}\rangle$ of the effective four-fermion Hamiltonian due to exchange of W and Z bosons over the state describing the background medium. We have

$$\mathcal{H}_{eff} = \mathcal{H}_{CC} + \mathcal{H}_{NC} \text{ -------------------------------- (20)}$$

With

$$\mathcal{H}_{CC} = \frac{G_F}{\sqrt{2}}[\bar{\nu}_e\gamma^{\rho}(1-\gamma^5)\nu_e] \times [\bar{e}\gamma_\rho(1-\gamma^5)e],$$

$\mathcal{H}_{NC} = \frac{G_F}{\sqrt{2}}\sum_{l=e,\mu,\tau}[\bar{\nu}_l\gamma^{\rho}(1-\gamma^5)\nu_l] \times \sum_{b=e,p,n}[\bar{b}\,\gamma_\rho(g_V^b - g_A^b\gamma^5)b]$, where G_F is the Fermi constant, g_V^b and g_A^b are the vector and axial vector coupling constants of the various background particles and we have performed a Fierz reshuffling of the fields [7,12]. In the above equations, it is taken into account that normal matter does not contain muons and taus and, consequently, the CC interactions with the medium only affect electron neutrino propagation. For nonrelativistic unpolarized medium, one obtains

$$V_\alpha = A_{CC}\delta_{\alpha e} + A_{NC}, \text{ -------------------------------- (23)}$$

Where the CC contribution

$$A_{CC} = \sqrt{2}G_F(n_e - n_{\bar{e}}) \text{ ---------------------------- (24)}$$

is proportional to difference between the number densities of electrons and positrons. The NC contribution A_{NC} is equal for all active neutrino flavours and is given by

$$A_{NC} = \frac{G_F}{\sqrt{2}}(1 - 4s_W^2)[(n_p - n_{\bar{p}}) - (n_e - n_{\bar{e}})] - \frac{G_F}{\sqrt{2}}(n_n - n_{\bar{n}}), \text{ --------- (25)}$$

where $s_W \equiv sin\theta_W$ while n_p and $n_n(n_{\bar{p}}$ and $n_{\bar{n}})$ are the number densities of protons and neutrons (antiprotons and antineutrons), respectively.

In neutral matter, it necessarily holds $(n_e - n_{\bar{e}}) = (n_p - n_{\bar{p}})$ that implies that the first term in the r.h.s. of the above equation vanishes. Moreover, in the absence of sterile neutrinos, the neutral current contribution to the total Hamiltonian is proportional to the identity matrix. As a consequence, it only introduces an overall unobservable phase factor in the evolution of $\nu^{(f)}(t)$ and, thus, can be neglected.

Finally, the evolution equation for antineutrinos is obtained by replacing $U \to U^*$ in equation (16) and $V \to -V$ in the equation (18). We, thus, understand that CP- violating effects are absent in neutrino oscillations, if the mixing matrix is real (i.e.,$U = U^*$) and neutrinos propagate in vacuum or in a CP-symmetric medium (i.e., V=0).

2.2 Oscillations in the Vacuum and in the matter

Let us assume that a neutrino flavour ν_α is created at a time $t_0 = 0$. In the flavour eigenstate basis, this state is represented by a vector

$$\nu^{(f)}(0) = (a_e(0), a_\mu(0), a_\tau(0), \dots)^T \text{ ------------ (26)}$$

with components $\alpha_\beta(0) = \delta_{\beta\alpha}$. After a time interval t, the neutrino propagated to a distance $x \approx t$ and its flavour content has evolved according to

$$\nu^{(f)}(x) = S^{(f)}(x)\nu^{(f)}(0), \text{ ---------------------(27)}$$

where the evolution operator is given by

$$S^{(f)}(x) = T[\exp(-i\int_0^x dx' \, H^{(f)}(x'))] \text{ --------- (28)}$$

and T represents the time ordering of the exponential. In the presence of neutrino mixing and if the neutrino masses are not degenerate, the Hamiltonian $H^{(f)}$is not diagonal. Thus, flavour is not conserved and components $\beta \neq \alpha$ can appear as a result of the evolution. The probability to detect a neutrino flavour ν_β at a distance L from the neutrino production point is given by

$$P(\nu_\alpha \to \nu_\beta) = |a_\beta(L)|^2 = |S_{\beta\alpha}^{(f)}(L)|^2. \text{ ---------- (29)}$$

2.3 Vacuum Neutrino Oscillations

In vacuum, the neutrino Hamiltonian H is constant. The evolution operator can be explicitly calculated as

$$S^{(f)} = US^{(m)}U^\dagger, \text{ -------------------------- (30)}$$

where $S^{(m)}$is the evolution operator in the mass eigenstate basis given by

$$S^{(m)} = \text{diag}(\exp(i\phi_1), \exp(i\phi_2), \dots, \exp(i\phi_N)), \text{ -------------- (31)}$$

with $\phi_i = -m_i^2 x/2|\vec{p}|$. The probability to observe the oscillation $\nu_\alpha \to \nu_\beta$ over a distance L is thus given by

$$P(\nu_\alpha \to \nu_\beta) = \sum_{i,j}[U_{\beta i}U_{\alpha i}^* U_{\beta j}^* U_{\alpha j}]\exp(i\phi_{ij}), \text{ ------ (32)}$$

where $\phi_{ij} = [(m_j^2 - m_i^2)L]/2E$ and we considered that for a relativistic particle $E \approx |\vec{p}|$. The above expression can be recast in few alternative forms that are useful to discuss the property of neutrino oscillations. We get, for example,

$$P(\nu_\alpha \to \nu_\beta) = \sum_i |U_{\beta i}|^2 |U_{\alpha i}|^2 + 2Re[\sum_{i>j} U_{\beta i}U_{\alpha i}^* U_{\beta j}^* U_{\alpha j}\exp(i\phi_{ij})], \text{ ------ (33)}$$

which gives the oscillation probability as the sum of a constant and an oscillating term. The oscillating part averages to zero if the phases ϕ_{ij} vary over ranges $\Delta\phi_{ij} \gg 1$, as it can be due, for example, to a spread of the neutrino energy E and the neutrino baseline L. The constant part represents the "classical limit" that is obtained by neglecting interference among different components of the neutrino wave packet and by combining probabilities, rather than amplitudes, to derive $P(\nu_\alpha \to \nu_\beta)$.

Alternatively, we can write

$$P(\nu_\alpha \to \nu_\beta) = \delta_{\alpha\beta} - 4\sum_{i>j} Re[U_{\beta i}U_{\alpha i}^* U_{\beta j}^* U_{\alpha j}]sin^2\left(\frac{\phi_{ij}}{2}\right) - 2\sum_{i>j} Im[U_{\beta i}U_{\alpha i}^* U_{\beta j}^* U_{\alpha j}]\sin(\phi_{ij}) \text{------------------- (34)}$$

The first two terms in the r.h.s. of the above equation do not change for $U \to U^*$and describe the CP-conserving part of the neutrino oscillation probability. The last part, instead, changes sign introducing a difference between neutrino and antineutrino oscillation probabilities that can be quantified as

$$P(\bar{\nu}_\alpha \to \bar{\nu}_\beta) - P(\nu_\alpha \to \nu_\beta) = 4\sum_{i>j} Im[U_{\beta i}U_{\alpha i}^* U_{\beta j}^* U_{\alpha j}]\sin(\phi_{ij}). \text{ ------------(35)}$$

For $\alpha = \beta$, this term vanishes showing that CP asymmetry can be measured only in transitions between different neutrino flavours.

If we assume two neutrinos mixing, that is, we take only one non-vanishing mixing angle θ_{ij}in equation (8), the oscillation probability reduces to the well- known expression

$$P(\nu_\alpha \to \nu_\beta) = sin^2(2\theta_{ij})sin^2\left(\frac{\Delta m_{ij}^2 L}{4E}\right), \text{ --------- (36)}$$

where $\alpha \neq \beta$ and the involved flavours depend on the mixing angle θ_{ij}(an angle $\theta_{12} \neq 0$ induces $\nu_e \to \nu_\mu$oscillations; $\theta_{31} \neq 0$ induces $\nu_e \to \nu_\tau$oscillations; $\theta_{23} \neq 0$ induces $\nu_\mu \to \nu_\tau$ oscillations). The survival probability for the case $\alpha = \beta$ can be simply deduced by considering that, due to unitarity of mixing matrix, it always holds $\sum_\beta P(\nu_\alpha \to \nu_\beta) \equiv 1$that, in this specific case, gives

$$P(\nu_\alpha \to \nu_\beta) = 1 - sin^2(2\theta_{ij})sin^2\left(\frac{\Delta m_{ij}^2 L}{4E}\right), \text{ --------(37)}$$

Equation (36) describes an oscillating function of L. The amplitude of the oscillation is determined by $sin^2(2\theta_{ij})$ while the oscillation length is given by

$$L_{ij} = \frac{4\pi E}{|\Delta m_{ij}^2|} = 2.48\frac{E[MeV]}{|\Delta m_{ij}^2[eV^2]|}m. \text{ ---------------- (38)}$$

The oscillation probabilities are unchanged when $\Delta m_{ij}^2 \rightarrow -\Delta m_{ij}^2$ or $\theta_{ij} \rightarrow \frac{\pi}{2} - \theta_{ij}$ showing that two neutrino oscillations in vacuum do not probe the hierarchy of the masses m_i and m_j (i.e., the states ν_i and ν_j can be interchanged with no effect on equation (36) and (37)). In the three-neutrino case, useful expressions can be derived in the approximation of one dominant mass scale (i.e., $\Delta m_{21}^2 \ll |\Delta m_{31}^2| \approx |\Delta m_{32}^2|$) which is motivated by the fact that the mass difference required to explain the atmospheric neutrino anomaly is much larger than that required to solve the solar neutrino problem. In this assumption (note that, due to CPT-invariance, it holds $P(\nu_\beta \rightarrow \nu_\alpha) = P(\bar{\nu}_\alpha \rightarrow \bar{\nu}_\beta)$) one gets

$P(\nu_e \rightarrow \nu_\mu) = s_{23}^2 sin^2(2\theta_{31})S_{23} + c_{23}^2 sin^2(2\theta_{12})S_{12} - P_{CP}$, ---------- (39)

$P(\nu_e \rightarrow \nu_\tau) = c_{23}^2 sin^2(2\theta_{31})S_{23} + s_{23}^2 sin^2(2\theta_{12})S_{12} + P_{CP}$, ----------- (40)

$P(\nu_\mu \rightarrow \nu_\tau) = c_{31}^4 sin^2(2\theta_{23})S_{23} - s_{23}^2 c_{23}^2 sin^2(2\theta_{12})S_{12} - P_{CP}$, ------------ (41)

where, following [9], we adopted the notation $S_{23} = sin^2(\Delta m_{32}^2 L/4E)$ and $S_{12} = sin^2(\Delta m_{21}^2 L/4E)$ and we set $\theta_{31} = 0$ in the coefficients of the S_{12} terms. The CP-violating part P_{CP}, which enters with opposite sign in the corresponding expressions for antineutrinos, is given by

$P_{CP} = 8J sin\left(\frac{\Delta m_{21}^2 L}{4E}\right) sin^2\left(\frac{\Delta m_{31}^2 L}{4E}\right)$, -------------------- (42)

where $J = \frac{1}{8}\sin(2\theta_{12})\sin(2\theta_{23})\sin(2\theta_{31})\cos(\theta_{13})\sin(\delta)$, --------- (43)

showing that CP violation is observed in neutrino oscillations only if all the angles and all the mass differences are nonvanishing. The magnitude of CP violating effects depends on the phase δ, being maximal for $\delta = \frac{\pi}{2}$ and $\delta = \frac{3\pi}{2}$. The survival probabilities $P(\nu_\alpha \rightarrow \nu_\alpha) = P(\bar{\nu}_\alpha \rightarrow \bar{\nu}_\alpha)$ are given by [9]

$P(\nu_e \rightarrow \nu_e) = 1 - sin^2(2\theta_{31})S_{23} - c_{31}^4 sin^2(2\theta_{12})S_{12}$, ------------------ (44)

$P(\nu_\mu \rightarrow \nu_\mu) = 1 - 4c_{31}^2 s_{23}^2(1 - c_{31}^2 s_{23}^2)S_{23} - c_{23}^4 sin^2(2\theta_{12})S_{12}$, -------(45)

$P(\nu_\tau \rightarrow \nu_\tau) = 1 - 4c_{31}^2 c_{23}^2(1 - c_{31}^2 c_{23}^2)S_{23} - s_{23}^4 sin^2(2\theta_{12})S_{12}$, -------- (46)

We note that, at this level of approximation, there is no sensitivity to neutrino hierarchy since the oscillation probabilities do not depend on the sign of Δm_{31}^2. Moreover, in the limit $\theta_{31} \rightarrow 0$, the "atmospheric" mass scale Δm_{32}^2 does not produce observable effects on electron neutrino oscillations that can be regarded as two neutrino oscillations, driven by the "solar" mass difference Δm_{21}^2, between ν_e and the mixed state $\nu_{\mu\tau} = c_{23}\nu_\mu - s_{23}\nu_\tau$. This conclusion also holds in presence of matter.

2.4 Neutrino Oscillations in Matter

The evolution of neutrinos in matter is complicated by the fact that the properties of the medium can change along the neutrino trajectory, thus giving a nonconstant Hamiltonian. The evolution equation is expressed as

$$i\frac{d\nu^{(f)}(x)}{dx} = \left[H_{vac}^{(f)} + V^{(f)}(x)\right]\nu^{(f)}(x), \text{ -------------(47)}$$

where, we neglect sterile neutrinos, the only nonvanishing entry of the matrix $V^{(f)}(x)$ is

$$\left(V^{(f)}\right)_{ee} = \pm\sqrt{2}G_F n_e(x). \text{ ------------------------ (48)}$$

Here, the "+" sign refers to neutrinos while the "−" sign refers to antineutrinos. In the above equations, we omitted the NC contribution to matter potential that is proportional to the identity matrix. We also assumed that the number density of positrons is negligible. It is convenient to diagonalize the Hamiltonian at each point of space and discuss the evolution on the basis of the *local mass eigenstates* defined by the following relation:

$$\nu^{(f)}(x) \equiv \widetilde{U}(x)\nu^{(\widetilde{m})}(x), \text{ ------------------------------- (49)}$$

where $\widetilde{U}(x)$ is the unitary matrix that gives

$$H_{vac}^{(f)} + V^{(f)}(x) = \frac{1}{2E}\widetilde{U}(x)\widetilde{M}^2(x)\widetilde{U}^\dagger(x), \text{ ------------- (50)}$$

with

$$\widetilde{M}^2(x) = \mathrm{diag}(\widetilde{m}_1^2(x), \widetilde{m}_2^2(x), \ldots, \widetilde{m}_N^2(x)). \text{ ---------- (51)}$$

On this basis, the evolution equation becomes

$$i\frac{d\nu^{(\widetilde{m})}(x)}{dx} = \left[\frac{\widetilde{M}^2}{2E} - i\widetilde{U}^\dagger(x)\frac{d\widetilde{U}(x)}{dx}\right]\nu^{(\widetilde{m})}(x). \text{ ------------- (52)}$$

We see that the nondiagonal entries, which may cause the transitions between the local mass eigen states, are proportional to the derivative of $\widetilde{U}(x)$ whose magnitude is essentially determined by the rate of change of the electrons number density in the background medium. This observation can be used to introduce the so-called *adiabatic* approximation that applies with good accuracy to the case of solar neutrino oscillations. Let us indicate with $\widetilde{L}_{ij} \approx 4\pi E/|\Delta\widetilde{m}_{ij}^2|$ the length scale over which the components of the neutrino wave packet with masses $\widetilde{m}_i$ and $\widetilde{m}_j$ acquire a phase difference $\Delta\phi_{ij} = 2\pi$. If we assume that the various $\widetilde{L}_{ij}$ are much smaller than the distance over which the medium changes its properties

$D \equiv (d\ln n_e(x)/dx)^{-1}$, the second term in the r.h.s. of equation (52) can be neglected. Thus, the components of the vector $\nu^{(\widetilde{m})}(x)$ remain constant (in magnitude) during the evolution, even if the decomposition of $\nu^{(\widetilde{m})}(x)$ in the flavour basis changes along the neutrino trajectory as a result of the variations of n_e. If the length scales $\widetilde{L}_{ij}$ are also much smaller than the baseline L over which neutrinos propagate, the oscillation probabilities $P(\nu_\alpha \rightarrow \nu_\beta)$ only depends on the properties of $\widetilde{U}(x)$ at the production point x_p and at the detection point x_d. They can be, in fact, deduced by incoherently combining probabilities of production and detection, obtaining

$$P(\nu_\alpha \rightarrow \nu_\beta) = \textstyle\sum_i \left|\widetilde{U}_{\alpha i}(x_p)\right|^2 \left|\widetilde{U}_{\beta i}(x_d)\right|^2. \text{ -----------(53)}$$

We now consider the specific case of ν_e produced by nuclear reactions occurring at the centre of the sun. Let us calculate the electron neutrino survival probability, by first considering a two neutrinos scenario in which only $\theta_{12} \neq 0$. The effective mixing angle in matter $\widetilde{\theta}_{12}$ can be calculated as

$$\sin(2\widetilde{\theta}_{12}) = \frac{\sin(2\theta_{12})}{\sqrt{sin^2(2\theta_{12}) + C^2}}, \text{ -------------------- (54)}$$

while the difference between the effective neutrino masses is given by

$$\Delta\widetilde{m}_{21}^2 \equiv \widetilde{m}_2^2 - \widetilde{m}_1^2 = \Delta m_{21}^2\sqrt{sin^2(2\theta_{12}) + C^2}, \text{ ----- (55)}$$

with

$$C(x) = \cos(2\theta_{12}) - \frac{2\sqrt{2}G_F n_e(x)E}{\Delta m_{21}^2}. \text{ -------------- (56)}$$

Matter effects break the degeneracies $\Delta m_{21}^2 \to -\Delta m_{21}^2$ and $\theta_{12} \to \frac{\pi}{2} - \theta_{12}$, probing the hierarchy in the 1-2 neutrino sector. In particular, $\Delta m_{21}^2 > 0$ and $\theta_{12} < \frac{\pi}{4}$, the system has a resonance. There exists, in fact, a value of the electron number density, defined by the following condition:

$$\Delta m_{21}^2 \cos(2\theta_{12}) = 2\sqrt{2}G_F n_e E, \text{ ----------------- (57)}$$

for which the local mixing is maximal(i.e.,$\tilde{\theta}_{12} = \frac{\pi}{4}$) while the mass difference $\Delta\tilde{m}_{12}^2 = \Delta m_{12}^2 \sin(2\theta_{12})$. As it was discussed by [5,6], if the resonance region is sufficiently wide, it is possible to achieve a total conversion of ν_e into neutrinos of different flavours.. This mechanism is called the MSW *effect*. Considering that the electron density in the Sun is $n_e \leq 10^{26} cm^{-3}$ and the typical solar neutrino energies are $E \approx 1MeV$, the resonance condition requires $\Delta m_{21}^2 \cos(2\theta_{12}) \leq 10^{-5} eV^2$.

The evolution equation in the local mass eigenstate basis becomes

$$i\frac{d\nu^{(\tilde{m})}(x)}{dx} = \left[\frac{1}{2E}\begin{pmatrix}\tilde{m}_1^2 & 0\\ 0 & \tilde{m}_2^2\end{pmatrix} + i\begin{pmatrix}0 & -\frac{d\tilde{\theta}_{12}}{dx}\\ \frac{d\tilde{\theta}_{12}}{dx} & 0\end{pmatrix}\right] \times \nu^{(\tilde{m})}(x),$$

-------------------- (58)

and the adiabaticity condition can be explicitly expressed as

$$\gamma(x) \gg 1, \text{ ---------------------------------59)}$$

where the *adiabaticity parameter* γ is given by the ratio between the differences of diagonal elements and off-diagonal elements of equation (58):

$$\gamma = \left|\frac{\Delta\tilde{m}_{21}^2/4E}{d\tilde{\theta}_{12}/dx}\right| \text{ --------------------------------(60)}$$

If the condition (59) is fulfilled, the electron neutrino survival probability can be calculated through equation (53). We get

$$P(\nu_e \to \nu_e) = \frac{1}{2} + \frac{1}{2}\cos(2\tilde{\theta}_{12})\cos(2\theta_{12}), \text{ ------- (61)}$$

where $\tilde{\theta}_{12}$ indicates the mixing angle at neutrino production point and we assumed that neutrinos are detected in vacuum.

In order to understand the specific features of $P(\nu_e \to \nu_e)$, it is useful to define a transition energy E^*, given by:

$$E^* = \frac{\Delta m_{21}^2 cos2\theta_{12}}{2\sqrt{2}G_F n_{e,\odot}}, \text{ ------------------------------(62)}$$

where $n_{e,\odot}$ is the electron number density at the centre of the sun. For $E \ll E^*$, matter effects are negligible and equation (61) reduces to

$$P(\nu_e \to \nu_e) = 1 - \frac{1}{2}sin^2(\theta_{12}) \text{ --------------(63)}$$

which, in fact, corresponds to vacuum averaged neutrino oscillations. For $E \gg E^*$, matter potential becomes dominant so that the "heaviest" mass eigenstates in the centre of the Sun coincide with ν_e. As a consequence, we obtain $\cos(2\tilde{\theta}_{12}) = -1$ and

$$P(\nu_e \to \nu_e) = sin^2(\theta_{12}) \text{ ---------------------(64)}$$

For the value of θ_{12} and Δm_{21}^2 currently favoured by neutrino oscillation analysis, the transition energy E^* is approximately $E^* \approx 1.2$MeV.

The violations of adiabaticity can be taken into account by introducing the crossing probability P_C that represents the probability of a transition between local mass eigenstates during neutrino evolution. If $P_C \neq 0$, the electron neutrino survival probability becomes

$$P(\nu_e \to \nu_e) = \frac{1}{2} + \left(\frac{1}{2} - P_C\right)\cos(2\tilde{\theta}_{12})\cos(2\theta_{12}) \text{ ----(65)}$$

There are different approaches to calculate P_C. For several cases of interest, the following expression holds. [9,13,14]

$$P_C = \frac{\exp(-(\frac{\pi}{2})\tilde{\gamma}F) - \exp(-(\frac{\pi}{2})\tilde{\gamma}(F/sin^2\theta_{12}))}{1 - \exp(-(\frac{\pi}{2})\tilde{\gamma}(F/sin^2\theta_{12}))}, \text{ ---------(66)}$$

where $\tilde{\gamma}$ is the minimal value of $\gamma(x)$ along the neutrino trajectory in the presence of a resonance, one can often approximate $\tilde{\gamma} \approx \gamma_{res}$ is the value of $\gamma(x)$ at the resonance point [7,9] and the parameter F depends on the adopted electron density profile. In particular, for an exponential density profile $n_e \propto \exp(-x)$, which is a good approximation for solar neutrinos, one has $F = 1 - tan^2\theta_{12}$.

In the case of three mixed neutrinos, the above picture has to be modified to take into account the possibility that $\theta_{23} \neq 0$ and $\theta_{13} \neq 0$. Since the matter potentials are equal for muon and tau neutrinos, the rotation $R(\theta_{23})$ in equation (8) can be reabsorbed in the "mixed" basis $\{|\nu_e\rangle, c_{23}|\nu_\mu\rangle - s_{23}|\nu_\tau\rangle, s_{23}|\nu_\mu\rangle + c_{23}|\nu_\tau\rangle\}$. This shows that, when $\theta_{13} = 0$, electron neutrinos experience two neutrino oscillations to a mixed state $|\nu_{\mu\tau}\rangle = c_{23}|\nu_\mu\rangle - s_{23}|\nu_\tau\rangle$ and, thus, the electron neutrino survival probability is unchanged. In the presence of $\theta_{13} \neq 0$, we have instead non trivial modifications due to the fact that the state $|\nu_e\rangle$ mixes with the state $|\nu_3\rangle$ being in fact $|\langle\nu_e|\nu_3\rangle| = s_{13}$. By repeating the previous calculations, we get

$$P(\nu_e \to \nu_e) = sin^4(\theta_{13}) + cos^4(\theta_{13}) \times \left[\frac{1}{2} + \left(\frac{1}{2} - P_C\right)\cos(2\tilde{\theta}_{12})\cos(2\theta_{12})\right] \text{ ---------(67)}$$

where it is assumed that the matter effects negligibly modify the θ_{13} mixing angle (i.e., $\theta_{13} \approx \tilde{\theta}_{13}$).

We finally remark that the above expression applies to solar neutrinos detected during the day, since these neutrinos do not cross the Earth to reach the detector. Matter effects due to the propagation across the Earth can modify equation (67) by introducing a day-night modulation whose magnitude depends on the specific values of mass and mixing parameters.

3. Experimental Status

The landmark discovery that neutrinos have mass and can change flavour as they propagate. This process is called neutrino oscillation [13-18]. It has opened up a rich array of theoretical and experimental questions being actively pursued today. Neutrino oscillation remains the most powerful experimental tool for addressing many of these questions, including whether neutrinos violate charge-parity (CP) symmetry, which has possible connections to the unexplained preponderance of matter over antimatter in the Universe [19-23]. Oscillation measurements also probe the mass-squared differences between the different neutrino mass states, Δm^2, whether there are two light states and a heavier one (normal ordering) or vice versa (inverted ordering), and the structure of neutrino mass and flavour mixing [24]. Here we carry out the first joint analysis of datasets from NOvA [25] and T2K [26], the two currently operating long-baseline neutrino oscillation experiments (hundreds of kilometres of neutrino travel distance), taking advantage of our complementary experimental designs and setting new constraints on several neutrino sector parameters. This analysis provides new precision on the Δm^2_{32} mass difference, finding $2.43^{+0.04}_{-0.03} \times 10^{-3} eV^2$in the normal ordering and $-2.48^{+0.03}_{-0.04} \times 10^{-3} eV^2$in the inverted ordering, as well as a 3σ interval on δ_{CP} of [−1.38π, 0.30π] in the normal ordering and [−0.92π, −0.04π] in the inverted ordering. The data show no strong preference for either mass ordering, but notably, if inverted ordering were assumed true within the three-flavour mixing model, then our results would provide evidence of CP symmetry violation in the lepton sector.

The standard model of particle physics, extended to include neutrino mass, describes three-flavour eigenstates of neutrinos $(\nu_e, \nu_\tau, \nu_\mu)$ that are related to three mass eigenstates (ν_1, ν_2, ν_3) by the 3×3 complex Pontecorvo–Maki–Nakagawa–Sakata unitary mixing matrix U_{PMNS}[27-29]. This mixing, together with non-zero neutrino mass, allows for the phenomenon of neutrino oscillation, in which, during propagation, the flavour content of a neutrino evolves at a rate that depends on neutrino mass-squared splitting ($\Delta m^2_{ij} = m^2_i - m^2_j$) and the U_{PMNS} matrix elements. Apart from these oscillation parameters, the rate depends on neutrino energy E_ν and neutrino propagation distance L (baseline). Although experiments studying this process in recent decades have provided insights into the details of neutrino masses and mixings [24], many open questions remain.

The mixing matrix U_{PMNS} is typically parameterized in terms of three mixing angles $(\theta_{12}, \theta_{13}, \theta_{23})$ and at least one complex phase δ_{CP}[24]. It is unknown whether $\sin\delta_{CP}$ is non-zero; if it is, neutrinos—and thus leptons—violate charge-parity (CP) symmetry and thereby provide a source of matter–antimatter asymmetry in nature [17], which is of great interest given the connection between CP violation and the unexplained matter dominance in the Universe [19-23]. Separately, oscillation experiments have established that the mass-squared splitting Δm^2_{32} is roughly 30 times larger in magnitude than Δm^2_{21}, but the sign of the former is at present unknown. That is, ν_3 may be heavier or lighter than the $\nu_1 - \nu_2$ pair, with these two options termed, respectively, the normal ($\Delta m^2_{32} > 0$) and inverted ($\Delta m^2_{32} < 0$) mass orderings. Knowledge of the mass ordering can constrain experimental searches and theory development in a wide range of physics, including absolute neutrino mass measurements [30], neutrinoless double beta decay searches to investigate the nature of neutrino mass [31], models of supernova explosion and detection [32-33], and the cosmological evolution evidenced in cosmic micro wave background and large-scale structure measurements [34]. For the mixing angles, current data suggest θ_{23} is near 45°, a notable value hinting at a μ/τ flavour symmetry [29]. Improved precision on this and other mixing angles is essential for gaining a clearer view of flavour mixing and to probe the validity of the three-flavour model.

Long-baseline accelerator neutrino oscillation experiments are well suited to address the above questions. In these, a high-intensity neutrino beam enriched in muon neutrinos (ν_μ) or muon antineutrinos ($\bar{\nu}_\mu$) is produced at a particle accelerator and directed through the crust of Earth towards a massive far detector located hundreds of kilometres away. It is to be noted that that the word 'neutrino' is used to mean both neutrino and antineutrino unless stated otherwise. The far detector measures the event rates of ν_μ and ν_e – the latter primarily from $\nu_\mu \rightarrow \nu_e$ oscillation – as a function of neutrino energy, from which the above oscillation parameters can be determined. These experiments use near detectors, sited a short distance from the beam source, in which oscillation effects are negligible and a very high neutrino event rate can be measured. The near detectors provide vital control measurements that substantially mitigate large systematic uncertainties in the initial neutrino flux, neutrino-on-nucleus interaction cross- sections and in some cases detector response. The impact of mass ordering and δ_{CP} on event rates have been shown in the fig.01

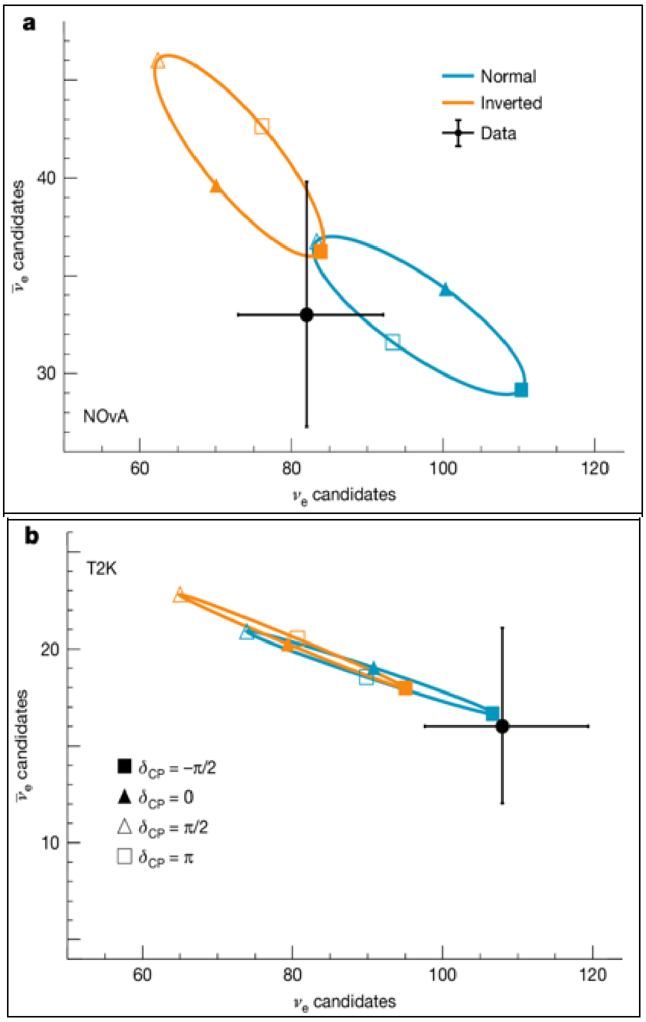

a, b, A bi-event plot that shows experimental sensitivity to neutrino mass ordering and δ_{CP}, with panels representing the NOvA(**a**) and T2K(**b**) cases. Black points with 1σ Poisson statistical error bars show the total number of ν_e and $\bar{\nu}_e$ candidates selected in the far detectors. The oval parametric curves trace out predicted numbers of events under the normal(blue) or inverted(orange) mass ordering assumption as the parameter δ_{CP} varies from -π to π. Four specifics δ_{CP} values are labelled for reference. All other oscillation parameters are kept fixed in graphic.

Two such experiments are in operation today, T2K and NOvA. Each experiment uses a narrow-band off axis beam, whose peak energy is near the first oscillation maximum, $sin^2\left(\frac{\Delta m_{32}^2 L}{4E}\right) \approx 1$, at the far detector. Note that natural units, where $\hbar = c = 1$ are used throughout. T2K uses an approximately 0.6 GeV neutrino beam from J-PARC in Tokai, Japan, and the 50-kt Super-Kamiokande water Cherenkov detector for its far detector located 295 km away [25]. In the United States, an approximately 2 GeV beam of NOvA is produced at Fermilab near Chicago, and the 14-kt tracking calorimeter far detector is located 810 km away in northern Minnesota.

We present here a combined analysis of the datasets from T2K and NOvA. This combination takes advantage of marked complementarity in the sensitivities of the two experiments to the oscillation parameters. In particular, the $\nu_\mu \rightarrow \nu_e$ oscillation probability is a function of both δ_{CP} and the neutrino mass ordering.

As shown in Fig. 1a, there is stronger separation between the mass ordering ovals for NOvA, because of higher beam energies, but as the NOvA data lie near the overlap of the ellipses, there can be ambiguity as to which ordering is correct and which values of $\delta_{CP}$are preferred. By contrast, T2K has less sensitivity to the mass ordering, but points with similar values of δ_{CP} in each hierarchy sit close to one another, and the data lie closest to $\delta_{CP} = -\frac{\pi}{2}$, regardless of mass ordering. Combining these datasets can provide simultaneous mass ordering and δ_{CP} information with substantially less ambiguity, maximizing the use of current data and informing data-taking strategies for current and future experiments.

This discussion points to a more general observation that the oscillation parameters of interest represent a highly correlated multidimensional space. The analysis reported here calculates a joint Bayesian posterior, using the likelihoods of the experiments defined over the full parameter space. Moreover, we use the full suite of analysis tools from both experiments: detector response models, neutrino energy estimators, near-detector measurements and systematic uncertainties, all within a unified framework for statistical inference. This level of integration is the first for accelerator neutrino experiments, to our knowledge.

The posterior calculation is based on detailed parameterized models of the neutrino flux, cross-sections and detectors that predict the binned spectra of neutrino events in each of our selected samples as a function of the oscillation parameters and a large number of nuisance parameters mostly related to systematic uncertainties in the models. A likelihood is constructed from Poisson probability terms describing the compatibility between the prediction and the observed data in bins of relevant variables. Prior probabilities are set on all parameters as detailed in the methods.

Both T2K and NOvA have software that explores the posterior using Markov chain Monte Carlo (MCMC) methods, (ARIA for NOvA and MaCh3 for T2K). By containerizing the likelihood and prior portions of the code, we can construct and analyse the joint posterior using either of the original MCMC frameworks, in spite of the very different software environments involved. For each fitting framework, ARIA or MaCh3, the native likelihood and priors of the fitter are calculated directly, whereas the likelihood and priors of other experiments are accessed using the software container. In this way, either framework can be used, providing valuable redundancy and thus cross-checks of all statistical inferences.

Although a single set of oscillation parameters naturally applies to both experiments in the joint posterior, the treatment of the many nuisance parameters related to systematic uncertainties is more subtle. Both measurements of the oscillation parameters at present have statistical uncertainties larger than the systematic uncertainties, but the latter are not negligible. We thoroughly surveyed the flux, cross-section and detector models and their systematic uncertainties to determine whether correlations between the experiments affect the analysis at a significant level. Our conclusions from this effort are summarized in the following paragraphs.

Both T2K and NOvA use beams produced by directing accelerated protons onto graphite targets. The hadrons are charge-selected with magnetic horns: positively charged hadrons decay to produce neutrinos, and negatively charged hadrons produce antineutrinos. Many uncertainties on these beam fluxes stem from processes unrelated between the two experiments, for example, the alignment of beam components. Yet, uncertainties on the rate of hadron production in the graphite targets are substantial, and the underlying physics is the same. However, the two experiments use proton beams of different energies (30 GeV for T2K and 120 GeV for NOvA), and the external datasets used to tune the hadron production models of both experiments are different. Moreover, the ultimate impact of flux uncertainties on far-detector predictions in NOvA is much smaller than other uncertainties. We, therefore, conclude that at current experimental exposures, the flux uncertainties of the two experiments need not be correlated.

Given the different detector technologies involved, most detector-related uncertainties are independent between the experiments. Furthermore, the very different energy estimation techniques used, combined with model tuning and uncertainty estimation using in situ calibration samples in each experiment, including for the lepton and neutron energy scales, lead to independence between the two detector uncertainty models. We conclude that there are no significant correlations in the detector models.

For neutrino-on-nucleus cross-sections, the underlying physics is the same; in many cases, the same external datasets are used by both experiments to tune and set prior uncertainties on model parameters. Thus, cross-section model correlations are expected. However, in the specific case of NOvA and T2K, the description of this physics differs markedly. The simulation packages differ, the physical models implemented in them differ in many places, the parameterizations differ almost entirely, and customized tunings are necessary and applied, given the specific energies of the experiments, detector technologies and approaches to systematic uncertainty mitigation.

Proper correlations between experiments could be implemented by starting from a common cross-section model spanning different energy ranges and able to describe both the leptonic and hadronic parts of the final state. A joint description is not yet mature and is one of the focuses of the community in the years to come. Given the differences in the models, a direct mapping of their parameters was deemed not practical at this time. Instead, we studied whether neglecting these correlations could appreciably affect our measurements of the oscillation parameters. The studies are limited to our current experimental exposures and models and would need re-evaluation if applied to any other context.

First, we assessed whether correlations between single systematic parameters in our models could have a substantial impact on our results. For each of Δm_{32}^2 ,θ_{23} and δ_{CP}, we identified the systematic parameter in each experiment with the largest impact on the measurement of that oscillation parameter. Then, regardless of whether those two systematic parameters made physical sense to correlate, we performed fits to simulated pseudo-data with the parameters fully correlated, uncorrelated and fully anticorrelated. Details of these studies, including how we identified the most impactful parameters, are shown in the methods. In summary, we saw no case in which the choice of correlation of individual systematic parameters significantly affected the oscillation parameter measurements.

Checking individual parameters does not rule out effects from a mix of systematic parameter variations that combine to produce a net effect that is larger and possibly more degenerate with oscillation effects, representing a potential worst-case scenario for the analyses. Rather than seeking such a set of variations, we directly identified, or in some cases constructed, single systematic parameters for each experiment that have effects similar to each oscillation parameter of interest. We then adjusted the size of the priors on these 'nightmare' parameters such that their impact on the measurements is comparable to that of statistical errors and therefore larger than the net effect of all our regular systematic parameters combined. These nightmare parameters were added to our nominal uncertainty models to create augmented models, allowing us to study a case in which systematic effects are comparable to statistical uncertainty. Next, we constructed simulated pseudo-datasets with the nightmare parameters increased in both experiments by one standard deviation above their prior central values. These simulated pseudo-data were then fit three times using the augmented model: once with the nightmare parameters of the experiments fully correlated (matching the pseudo-data), once fully anticorrelated and finally uncorrelated. We find that the oscillation parameter constraints extracted in the fully correlated and uncorrelated cases have negligible differences. However, the incorrect anticorrelated case yields a large bias. We expect that with even larger systematic uncertainties, differences between the correlated and uncorrelated cases would eventually become relevant. However, this study indicates that we are not in such a regime with the current exposures and systematic uncertainties.

Given that no significant biases are seen from neglecting correlations between actual systematic parameters, and the only bias seen with the nightmare parameters comes not from neglecting a correlation but from adding an incorrect one, we choose in most cases to neglect the correlations between the systematic uncertainties of the two experiments. The one exception relates to the approximately 2% normalization uncertainties on all ν_e and events described. In this case, the uncertainties are implemented identically by T2K and NOvA, and we have correlated them.

We also perform studies in which the joint fit is tested against pseudo-data constructed with a set of discrete model variations not directly accessible using the nominal uncertainty models of the experiments. Similarly, we studied a secondary set of variations based on extrapolating the cross-section model of each experiment to the context of the other experiment. Predefined thresholds were used to establish that no substantive changes in the central values or interval widths of the oscillation parameters were seen under these tests, as described in the methods. Each experiment continues to investigate improvements in its cross-section models, and the studies described here would warrant repeating for larger data exposures and/or updated theoretical understanding. Continued theoretical and experimental effort in this direction is important.

We produce parameter estimations using the highest-posterior-density credible intervals and perform discrete hypothesis tests using the Bayes factor formalism. Conclusions related to CP conservation or violation,Δm_{32}^2 , $sin^2\theta_{23}$ and mass ordering have been tested to be robust under the alternative model variations described previously.

We find $sin^2\theta_{23} = 0.56^{+0.03}_{-0.05}$ without any assumptions on the ordering of the neutrino masses. The fit weakly prefers the upper octant of$sin^2\theta_{23} > 0.5$ over the lower octant with a Bayes factor of 3.5. Removing the reactor constraint gives no statistically significant preference for either octant (Bayes factor 1.2 for the lower octant compared with the upper octant). We also find $\Delta m_{32}^2 = 2.43^{+0.04}_{-0.03} \times 10^{-3} eV^2$ assuming the normal ordering and $\Delta m_{32}^2 = 2.48^{+0.03}_{-0.04} \times 10^{-3} eV^2$ assuming the inverted ordering. This is at present the smallest experimental uncertainty on $|\Delta m_{32}^2|$(Fig. 2), to our knowledge. This conclusion also applies when the reactor constraint is replaced by a flat prior.

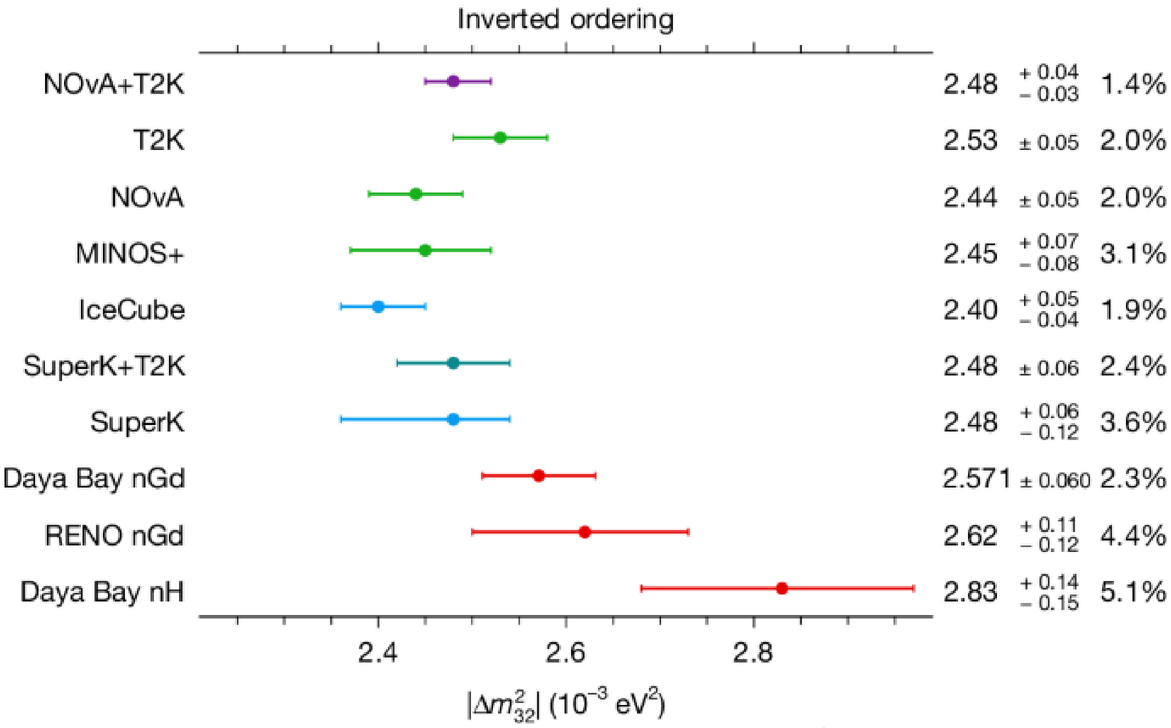

Figure 2: Experimental measurements of $|\Delta m^2_{32}|$

The measurements assume the inverted ordering preferred by this analysis.

4. Conclusion

Neutrino oscillations have transformed our understanding of particle physics, providing evidence for physics beyond the Standard Model. While the phenomenon is well established, critical questions remain unanswered. Resolving the mass hierarchy, measuring CP violation, and probing the absolute neutrino mass scale are among the most pressing challenges. Upcoming experiments promise to shed light on these mysteries, potentially revealing new physics and deepening our understanding of the Universe.

Acknowledgements

The author acknowledges the contributions of numerous experimental collaborations whose results have shaped the current understanding of neutrino physics.

References

[1] B. Pontecorvo, "Mesonium and anti-mesonium," *Soviet Physics JETP,* vol.6, p.429,1957.
[2] B. Pontecorvo, "Mesonium and anti-mesonium," *Journal of Experimental and Theoretical Physics,* vol.33, pp.549-551,1957.
[3] B. Pontecorvo, "Inverse beta processes and non - conservation of lepton charge," *Journal of Experimental and Theoretical Physics,* vol.34, p.247,1958.
[4] L. Wolfenstein, "Neutrino oscillations in matter," *Physical Review D,* vol.17, no.9, pp. 2369-2374,1978.
[5] S.P. Mikheyev and A. Yu. Smirnov, "Resonance amplification of oscillations in matter and spectroscopy of solar neutrinos," *Soviet Journal of Nuclear Physics,* vol.42, no.1, pp.913-917,1985.
[6] S.P. Mikheyev and A. Yu. Smirnov, "Resonant amplification of ν oscillations in matter and solar-neutrino spectroscopy," *Il Nuovo Cimento* C, vol.9, no.1, pp17-27,1986.
[7] C. Giunti and C.W. Kim, *Fundamentals of Neutrino Physics and Astrophysics,* Oxford University Press, New York, NY, USA, 2007.
[8] S.M. Bilenky, C. Giunti, and W. Grimus, "Phenomenology of neutrino oscillations," *Progress in Particle and Nuclear Physics,* vol.43, no.1, pp. 1-86, 1999.
[9] A. Strumia and F. Vissani, "Neutrino masses, mixings and …," http://arxiv.org/abs/hep-ph/0606054.
[10] J. Beringer, J.F. Arguin, R.M. Barnett et al., "Review of particle physics," *Physical Review D,* vol.86, no. 1, Article ID 010001,1528 pages, 2012.
[11] S.M. Bilenk, J. Hosek, and S.T. Petcov, "On oscillations of neutrinos with dirac and majorana masses," *Physics Letter B,* vol.94, no.4, pp.495-498,1980.
[12] M. Blennow and A.Y. Smirnov, "Neutrino propagation in matter," *Advances in High Energy Physics,* vol.2013, Article ID 972485, 33 pages, 2013.
[13] Fukuda, Y. et al. Evidence for oscillation of atmospheric neutrinos. Phys. Rev. Lett. 81, 1562–1567 (1998).
[14] Fukuda, S. et al. Determination of solar neutrino oscillation parameters using 1496 days of Super-Kamiokande-I data. Phys. Lett. B 539, 179–187 (2002).
[15] Ahmad, Q. R. et al. Measurement of the rate of $\nu + d \rightarrow p + p + e-$ interactions produced by 8B solar neutrinos at the Sudbury Neutrino Observatory. Phys. Rev. Lett. 87, 071301 (2001).
[16] Ahmad, Q. R. et al. Direct evidence for neutrino flavor transformation from neutral-current interactions in the Sudbury Neutrino Observatory. Phys. Rev. Lett. 89, 011301 (2002).
[17] Eguchi, K. et al. First results from KamLAND: evidence for reactor antineutrino disappearance. Phys. Rev. Lett. 90, 021802 (2003).

[18] An, F. P. et al. Observation of electron-antineutrino disappearance at Daya Bay. Phys. Rev. Lett. 108, 171803 (2012).
[19] Fukugita, M. & Yanagida, T. Barygenesis without grand unification. Phys. Lett. B 174, 45–47 (1986).
[20] Buchmüller, W., Peccei, R. D. & Yanagida, T. Leptogenesis as the origin of matter. Annu. Rev. Nucl. Part. Sci. 55, 311–355 (2005).
[21] Pascoli, S., Petcov, S. T. & Riotto, A. Connecting low energy leptonic CP violation to leptogenesis. Phys. Rev. D 75, 083511 (2007).
[22] Branco, G. C., Gonzalez Felipe, R. & Joaquim, F. R. Leptonic CP violation. Rev. Mod. Phys. 84, 515–565 (2012).
[23] Hagedorn, C., Mohapatra, R. N., Molinaro, E., Nishi, C. C. & Petcov, S. T. CP violation in the lepton sector and implications for leptogenesis. Int. J. Mod. Phys. A 33, 1842006 (2018).
[24] Particle Data Group et al. Review of particle physics. Prog. Theor. Exp. Phys. 2022, 083C01 (2022).
[25] Acero, M. A. et al. Improved measurement of neutrino oscillation parameters by the NOvA experiment. Phys. Rev. D 106, 032004 (2022).
[26] Abe, K. et al. Measurements of neutrino oscillation parameters from the T2K experiment using 3.6 × 1021 protons on target. Eur. Phys. J. C 83, 782 (2023).
[27] Maki, Z., Nakagawa, M. & Sakata, S. Remarks on the unified model of elementary particles. Prog. Theor. Phys. 28, 870–880 (1962).
[28] Pontecorvo, B. Neutrino experiments and the problem of conservation of leptonic charge. Zh. Eksp. Teor. Fiz. 53, 1717–1725 (1967).
[29] Mohapatra, R. N. et al. Theory of neutrinos: a white paper. Rep. Prog. Phys. 70, 1757 (2007).
[30] Formaggio, J. A., de Gouvea, A. L. C. & Robertson, R. G. H. Direct measurements of neutrino mass. Phys. Rep. 914, 1–54 (2021).
[31] Dolinski, M. J., Poon, A. W. P. & Rodejohann, W. Neutrinoless double-beta decay: status and prospects. Annu. Rev. Nucl. Part. Sci. 69, 219–251 (2019).
[32] Hansen, R. S. L., Lindner, M. & Scholer, O. Timing the neutrino signal of a galactic supernova. Phys. Rev. D 101, 123018 (2020).
[33] Horiuchi, S. & Kneller, J. P. What can be learned from a future supernova neutrino detection? J. Phys. G 45, 043002 (2018).
[34] Lesgourgues, J. & Pastor, S. Neutrino mass from cosmology. Adv. High Energy Phys. 2012, 608515 (2012).